Solar Energy 134 (2016) 228–235

Contents lists available at ScienceDirect

Solar Energy

journal homepage: www.elsevier.com/locate/solener

Martian Top of the Atmosphere 10–420 nm spectral irradiance database and forecast for solar cycle 24

Alfonso Delgado-Bonal [a,b,*], María-Paz Zorzano [b,c], F. Javier Martín-Torres [a,b]

[a] Instituto Andaluz de Ciencias de la Tierra (CSIC-UGR), Avda. de Las Palmeras n 4, Armilla, 18100 Granada, Spain
[b] Division of Space Technology, Department of Computer Science, Electrical and Space Engineering, Luleå University of Technology, Kiruna, Sweden
[c] Centro de Astrobiología (INTA-CSIC), Ctra. Ajalvir km. 4, Torrejón de Ardoz, 28850 Madrid, Spain

ARTICLE INFO

Article history:
Received 27 April 2015
Received in revised form 26 March 2016
Accepted 4 May 2016

Keywords:
Mars TOA
UV radiation
REMS
Space exploration

ABSTRACT

Ultraviolet radiation from 10 to 420 nm reaching Mars Top of the Atmosphere (TOA) and surface is important in a wide variety of fields such as space exploration, climate modeling, and spacecraft design, as it has impact in the physics and chemistry of the atmosphere and soil. Despite the existence of databases for UV radiation reaching Earth TOA, based in space-borne instrumentation orbiting our planet, there is no similar information for Mars. Here we present a Mars TOA UV spectral irradiance database for solar cycle 24 (years 2008–2019), containing daily values from 10 to 420 nm. The values in this database have been computed using a model that is fed by the Earth-orbiting Solar Radiation and Climate Experiment (SORCE) data. As the radiation coming from the Sun is not completely isotropic, in order to eliminate the geometrically related features but being able to capture the general characteristics of the solar cycle stage, we provide 3-, 7- and 15-days averaged values at each wavelength. Our database is of interest for atmospheric modeling and spectrally dependent experiments on Mars, the analysis of current and upcoming surface missions (rovers and landers) and orbiters in Mars. Daily values for the TOA UV conditions at the rover Curiosity location, as well as for the NASA Insight mission in 2016, and ESA/Russia ExoMars mission in 2018 are provided.

1. Introduction

Ultraviolet (UV) radiation covers the range from 10 to 400 nm of the electromagnetic spectrum and is usually divided into different channels with different implications for atmospheric sciences, engineering, biology and medicine. The determination of the solar UV radiation reaching the planets is of importance in a range of scientific and engineering disciplines, and it is a driving force of chemical, organic and biological evolution, being a key factor in climate modeling. Although UV radiation energy is less than 3% of all solar radiation reaching the Earth, and the total solar irradiance varies by about 0.1% during the course of the solar cycle, the spectral features change in the course of a solar cycle and these variations are highly significant in terms of its effects on climate modeling or biological responses. For example, photochemistry in the atmosphere is very sensitive to small changes in UV radiation, being this radiation the driver of ozone chemistry on Earth (Merkel et al., 2011) and one of the potential triggers of methane on Mars (Keppler et al., 2012).

The solar cycle is the periodic change in the Sun's activity with an average duration of about 11 years. During the cycle, the levels of solar radiation and ejection of solar material change, with visible manifestations such as the number of sunspots or flares. Those changes have implications in space weather, and on Earth's and other planets weather and climate. Fig. 1 shows the 11 years variability of the Sun measured by the Solar Radiation and Climate Experiment (SORCE) mission. The Total Solar Irradiance (TSI) is represented in W/m^2 from 2003 to 2014, showing the change in the irradiation from the Sun that reaches the Earth. The changes in the TSI are also accompanied by changes in individual wavelengths or spectral regions. Besides the 11 years cycle, aperiodic fluctuations are also a component of solar variation. Solar variability in the UV is a result of the growth and decay of active regions and other features on the Sun and are distributed unevenly over the surface of the Sun.

As the radiation reaching a planet is a dynamical feature, it is important to know the most precise values possible. The UV radiation has been monitored on Earth's surface and Top of the Atmosphere (TOA) extensively and treated as a key environmental and health parameter (Ghetti et al., 2006). One of the most complete Earth's TOA UV radiation databases available has been provided by the NASA Solar Radiation and Climate Experiment (SORCE)

* Corresponding author at: Instituto Andaluz de Ciencias de la Tierra (CSIC-UGR), Avda. de Las Palmeras n 4, Armilla, 18100 Granada, Spain.
E-mail address: alfonso.delgado-bonal@ltu.se (A. Delgado-Bonal).

http://dx.doi.org/10.1016/j.solener.2016.05.004
0038-092X/

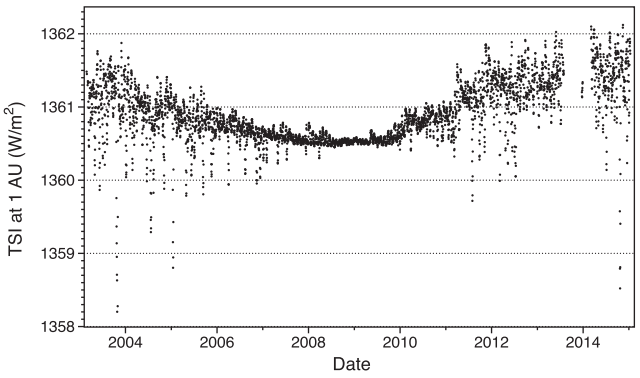

Fig. 1. Total Solar Irradiance (TSI) data in W/m^2 since 2003 to 2014 from SORCE mission at 1 AU.

experiment (Rottman et al., 2006). SORCE was launched in January 2003 and is still operating and measuring the total solar irradiance (TSI) and solar spectral irradiance from 1 nm to 2000 nm, accounting for 95% of the spectral contribution to the TSI.

Despite the existence of this and other databases for Earth, there are not available UV radiation databases for other planets, particularly Mars. To solve this lack of data, standard radiation spectra scaled for Mars have been used in atmospheric and engineering research, such as the Thuillier spectra (Thuillier et al., 2003), but these spectra do not allow to study cyclic variations in spectral irradiance on Mars.

On Mars, photochemistry is mainly driven by wavelengths lower than 200 nm, involving CO_2 and H_2O of the atmosphere. The martian atmosphere is composed by 98% of CO_2, which has absorption bands between 210 and 190 nm, and also between 180–135 nm and 125–120 nm. H_2O is also present in the martian atmosphere and its photolysis is the driver of ozone photochemistry for example. H_2O has absorption bands at 166.5 nm and 125 nm, although the 200 nm and 266 nm bands are also important; even lower wavelengths such as the 56 nm absorption band are important for photochemistry on Mars.

Wavelengths from 200 to 400 nm are also important in the study of other atmospheric compounds such as ozone, or to the analysis of dust and biology responses on Mars. The increment of UV-B (280–315 nm) is known to impair essential biological processes (Häder et al., 2007, 2011). The UV-C (200–280 nm) radiation is specially harmful for living beings, causing high damage even in low doses (Lindberg and Horneck, 1991). This radiation is blocked in Earth's atmosphere mainly by oxygen and ozone, blocking the radiation at different wavelengths (the Hartley bands between 200 and 300 nm, the Huggins bands between 320 and 360 nm and the Chappuis bands between 375 and 650 nm). UV-B (280–315 nm) and UV-A (315–400 nm) radiation cause also damage to cells, and they are also biologically interesting because of their effects as photosynthesis inhibitors and their relation with carbon fixation (Boucher et al., 1994), among others.

The aim of this paper is to provide a daily UV radiation database for Mars TOA for Solar Cycle 24 (2008–2019) representative of the solar stage in the solar cycle and orbital position of the planet. For this purpose we have used the data from the SORCE mission and the UV model developed by Woods and Rottman (W–R) (Woods and Rottman, 2002) to compute the radiation reaching Mars TOA for solar cycle 24 (2008–2019) in the spectral range 10–420 nm with an step of $\Delta\lambda = 1$ nm interval. The model used in this paper was provided to us by Tom Woods.

This paper is distributed as follows. In Section 2 we explain the procedure followed to generate the UV database reaching the Martian Top of the Atmosphere. In Section 3 we present the main results of the model, as average values and as integrated values; in Section 3.1 we compare the modeled Mars TOA spectral irradiance with UV in-situ measurements taken by the instrument REMS (Rover Environmental Meteorological Station) onboard the Curiosity rover in Mars (Gómez-Elvira et al., 2012, 2014) and in Section 3.2 we provide values for locations of the upcoming surface missions to Mars. Finally, in Section 4 we summarize the results of the database, freely available at https://atmospheres.research.ltu.se/ in the resources section.

2. The model

The Solar Radiation and Climate Experiment (SORCE) mission was launched in 2003 to enable solar-terrestrial studies by providing precise daily measurements of the total solar irradiance (TSI) and the solar spectral irradiance (SSI) at wavelengths extending from the UV to the near infrared (1–2000 nm) (Rottman, 2005). The SORCE mission is still operating and is managed by the Laboratory for Atmospheric and Space Physics (LASP), University of Colorado. The SORCE database is publicly accessible at http://lasp.colorado.edu/lisird/sorce/.

The spectral range measured by the SORCE (1–2000 nm) includes UV radiation with an excellent precision (Rottman et al., 2006; Pankratz et al., 2005), and it has been used to validate models (Ball et al., 2011) and evaluate the effect of UV radiation variations on climate modeling (Ermolli et al., 2012). This data set includes measurements from the XUV Photometer System (XPS, 0.1–40 nm), the SOLar STellar Irradiance Comparison Experiment (SOLSTICE, 115–310 nm), and the Spectral Irradiance Monitor (SIM, 310–2400 nm). It is important to notice that the UV measurements from 310 to 2400 nm are unavailable since September 2010.

There are no similar missions orbiting Mars, so we have developed a model to provide values of the Mars TOA UV spectral irradiance for solar cycle 24 (2008–2019), between 10 and 420 nm. As solar cycle 24 is currently on-going, we have separated our database in two parts: the first part is based in SORCE data and provides values of past UV radiation on Mars from 2008 to 2013, and the second part is based on W–R model along with the predicted solar radio flux at 10.7 cm (F10.7 index) and covers the years 2014–2019.

The first section of the database is based on the extrapolation of the SORCE data to Mars TOA. Despite the fact that the SORCE database contains spectral irradiance values at 1 AU for almost every wavelength from 2008 to 2013, there are some gaps. These gaps include missing wavelengths in particular days, or the fact that SORCE mission has been deactivated during some days for maintenance; in this manuscript, we have used the full range of SORCE SSI data version L3 C24H at 20130729, but the database will be periodically updated with the newest datasets. As our intention is to provide a complete database for Mars, we have filled those gaps in the database with values from the Woods–Rottman (W–R) model.

The Woods–Rottman model was developed form UARS SOLSTICE data for the FUV wavelength range and feeds with the daily and monthly F10.7 index, being its calculations in general very precise. The solar radio flux at 10.7 cm (2800 MHz) has been used since 1947 and is an excellent indicator of solar activity. The F10.7 radio emissions are features of the chromosphere and the corona of the solar atmosphere, and it is correlated with the sunspot number as well as a number of ultraviolet and visible solar irradiance records. Measured on a day-to-day basis from the Earths surface, the F10.7 index has proven very valuable in specifying and forecasting space weather, and provides climatology of solar activity over the last six solar cycles.

Nowadays there are available a variety of models for the determination of the radiation values, and we have selected the W–R

model due to its simplicity and little information needed to run. As the W–R model is in general used in this paper to make predictions, the uncertainty in the values of the future F10.7 index is bigger than the possible pitfalls of the model.

The W–R model is also used to fill the gaps in the data. Although the W–R model gives very approximate values, when we compare the SORCE database with the results of the model, we obtain differences between them. In order to fill the gaps in the SORCE database, we have compared the values in the SORCE database with the values of the Woods–Rottman model during the period 2008–2013, and computed the mean deviation of the model at each wavelength.

Those mean deviations were used to correct the values of the W–R model and fill the gaps for those days in which the SORCE database lacks data, being able to reproduce the expected behavior of the curve. In the occasional cases where a value of the spectral irradiance is missing in all the SORCE database for a given wavelength, the mean deviation of the closest wavelength was used to correct the model. In this way, we obtain a complete database that can be extrapolated to Mars. In Fig. 2 we show an example of the integrated UV radiation between 220 and 280 nm computed with SORCE data (black line) and with the W–R model (blue line). It is possible to see that the SORCE database contains gaps in specific days and the line is dashed. Using the W–R model and the mean deviation, our database (red line) is able to reproduce the expected behavior and fill those gaps to have a continuous and smooth curve.

We have modeled the orbit of Mars to calculate its distance from the Sun as a function of Solar Longitude, the angle between Mars–Sun measured from the Northern Hemisphere (being the summer solstice Ls = 90, the autumn equinox Ls = 180, the winter solstice Ls = 270 and the spring equinox Ls = 360). One of the main parameters determining the spectral irradiance on Mars TOA is the position of the planet in the orbit. Unlike the Earth, Mars orbit is not close to a circular orbit (eccentricity 5.58 times greater), which implies a change in the TSI between Mars aphelion and perihelion of about 45%. This implies that the relative differences of the radiation reaching the planet during an orbit are larger than on Earth, creating a larger difference among season temperatures and irradiances.

Once the distance is determined, the spectral irradiance reaching it is extrapolated as:

$$I_\lambda = I_{\lambda,0} \cdot \frac{1}{R^2_{Mars}} \tag{1}$$

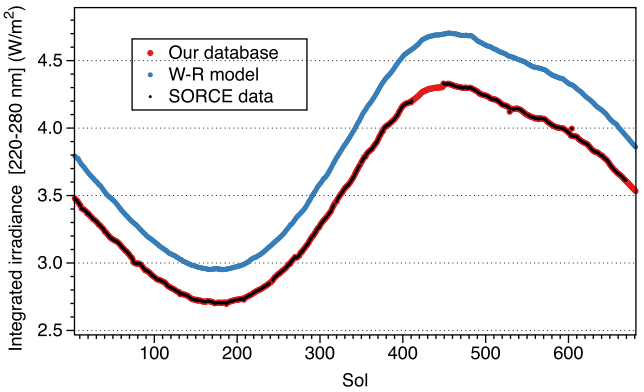

Fig. 2. UV integration between 220 and 280 nm using the SORCE data (black line), W–R model (blue line) and our database (red line). It is possible to see a gap in the SORCE data that is filled in out database using the W–R model and the mean deviation of the previous days. (For interpretation of the references to color in this figure legend, the reader is referred to the web version of this article.)

where $I_{\lambda,0}$ is the spectral irradiance at 1 AU measured by SORCE and R^2_{Mars} is the instantaneous Sun–Mars distance expressed in AU. The instantaneous position of Mars in its orbit can be determined using its semi-major axis and eccentricity (Levine et al., 1977). The irradiance at a particular position on Mars TOA is calculated as:

$$I_{\phi,\lambda} = I_\lambda \cdot \cos(z) \tag{2}$$

where ϕ is the latitude and z is the zenith angle of the incident solar radiation. The radiation reaching the martian TOA will depend on the latitude of the selected location and on the position of the planet in the orbit. These dependences are implicit in the zenith angle, which is calculated as:

$$\cos(z) = \sin(\phi)\sin(\delta) + \cos(\phi)\cos(\delta)\cos(h) \tag{3}$$

where δ is the declination, calculated as:

$$\delta = \arcsin(\sin(e) \cdot \sin(\mathrm{Ls})) \tag{4}$$

In summary, for the first section of the database (2008–2013) we have followed the following steps: (1) to model the orbit of Mars from 2008 to 2013; (2) to calculate the daily distance between Mars and the Sun; (3) to compute the spectral irradiance at 1 AU using the Woods–Rottman model with measured F10.7 data; (4) to estimate the mean deviation of the spectral irradiance between the model and SORCE data at each wavelength; (5) to use the Woods–Rottman values corrected by the mean deviation to fill the gaps in the SORCE database; (6) to compute the spectral irradiance reaching Mars TOA.

In addition to our calculations of the spectral irradiance for the period 2008–2013, we provide a prediction of the solar spectral irradiance reaching Mars TOA until 2019, based in the prediction of the solar flux and the position of the planet in its orbit. For that we use the accepted monthly average and daily F10.7 radio flux available at the NOAA Space Weather Prediction Center (SWPC) website (ftp://ftp.swpc.noaa.gov/pub/weekly/Predict.txt). The prediction of the F10.7 for solar cycle 24 is provided by the Solar Cycle Prediction Panel representing the National Oceanic and Atmospheric Administration (NOAA), the International Space Environmental Services (ISES), and NASA. In this paper we have used the Feb 2014 prediction; in the following versions of the database the more updated version will be used and specified.

The results of these calculations constitute the second part of our database, which has the intention to be a tool for current and future missions to Mars and for scientific studies of the planet. For the calculations of this second part (2013–2019), we have used the mean deviation between real data and the results of the code computed in the 2008–2013 interval to correct the values of the W–R model. The algorithm used for the second part of the database is: (1) to model the orbit of Mars from 2013 to 2019; (2) to calculate the daily distance between Mars and the Sun; (3) to compute the spectral irradiance at 1 AU using the Woods–Rottman model with predicted F10.7 data; (4) to correct the Woods–Rottman values with the mean deviation at each wavelength obtained in the first section of the database; (5) to compute the spectral irradiance reaching Mars TOA.

As a result of the model the UV spectral irradiance (10–420 nm) reaching Mars Top of the Atmosphere has been calculated in a daily basis for Solar Cycle 24 (years 2008–2019). A summary of the results and some examples of its application are presented in Section 3.

Solar radiation is not totally isotropic and contains daily features that are dependent on the geometrical location of the observer, such as solar storms or sunspots. These daily variations were measured by SORCE at the Earth's position, but not necessarily reached the martian atmosphere. In order to eliminate those daily variations but capture the global solar features at a particular stage

of the solar cycle, we provide values not only of the daily extrapolated spectral irradiance, but also the mean values of 3, 7 and 15 days. In this way, the users are able to choose those values that better fit their research interest, and obtain, in general, better results than using standard spectra.

3. Applications

In this section, we show the results of the model and examples of the use of the database. The radiation reaching the TOA is dependent on the position of the planet in the orbit, the latitude of the observer, and also depends on the stage of the Sun in the solar cycle. The position of the planet is determined by the solar longitude (Ls, Mars–Sun angle) measured from the northern hemisphere, which is Ls = 0 in vernal equinox. A summary of the results of the model for Ls 90, Ls 180, Ls 270 and Ls 360 for the maximum and the minimum of the solar cycle is presented in Tables 1–3. The starting point of the Solar Cycle 24 has been taken as the minimum value, the Martian year 29 (2008/2009), and we use the Martian year 31 (2012/2013) as maximum of this cycle.

The knowledge of the spectral irradiance allows the integration in spectral ranges. Tables 1 and 2 show the spectral integration of channels UV-C (200–280 nm), UV-B (280–315 nm) and UV-A (315–400 nm) for different Ls. The differences between the maximum and the minimum in UV radiation are relatively small over the year. These differences can be seen in Table 3.

To solve the lack of a martian UV database, Thuiller proposed two different generic spectra to be used in martian research, for the maximum and minimum of the solar cycle. With this database, we pretend to go further and expand the availability of data for the community. In Fig. 3 we compare the spectra generated with our model versus the generic Thuillier spectra. This figure underlines the need of using a database for different stages of the solar cycle instead of using generic spectra. Although the shapes of the spectra are quite similar, the spectral differences can be up to 50% of the intensity as a consequence of the Ca II K solar lines at 393 and 397 nm for example. The Ca II K line is formed by ionized calcium, which goes from the ground level to the first level; it provides important information on the large-scale magnetic field structure in the chromosphere and it is used to study the variation of the luminosity of the Sun and the detection of stellar activity cycles. These lines have a strong variability over the 11-years solar cycle and must be considered in atmospheric sciences and engineering research. In general, the variations are smaller than that, usually between 5% and 10%, but still important to be taken into account. These variations on UV radiation have, for example, the potential to produce changes on ozone chemistry (Merkel et al., 2011), which in turn has implications in water vapor and methane amount in the atmosphere of Mars. This database provides a tool to analyze those changes on Mars atmosphere that cannot be analysed using generic spectra.

3.1. Calculation of opacity after REMS/Curiosity data

The REMS UV sensor consists of one SiC photodiode dedicated to the UV spectrum 200–380 nm together with 5 filtered photodiodes for narrower band channels (Gómez-Elvira et al., 2012, 2014). During the day, as the Sun moves in the sky, the measured UV spectral irradiance varies from diffuse irradiance in the morning, to global irradiance close to noon (when the direct Sun beam is within the field of view of the photodiodes), and diffuse irradiance again in the afternoon. The downwelling solar UV irradiance interacts with the atmospheric molecules and dust as it goes from the top of the atmosphere to the surface. Variations in the downwelling irradiance can be used to characterize the properties of the atmosphere and for this a precise knowledge of the UV irradiance at TOA is critical. In particular the aerosol content of the atmosphere can be retrieved by measuring the opacity at a given wavelength (when this parameter is evaluated at visible wavelengths is usually referred to as optical depth):

$$\tau(\lambda)\cdot\cos(\mathrm{SZA}) = -\ln\frac{I_{dir}(\lambda)}{I^{S}_{TOA}(\lambda)} \quad (5)$$

Here SZA is the Solar Zenith Angle at the moment of observation. The above expression describes the exponential decay of the solar incident radiation at the Top Of the Atmosphere (TOA), $I^{S}_{TOA}(\lambda)$. Here $I_{dir}(\lambda)$ is the direct component of irradiance, i.e. the radiation that reaches the surface in the direct path from the Sun. Photons of the direct component have passed straightly through the atmosphere. The rest of the photons reaching the

Table 1
Total daily irradiances in the UV-C, UV-B and UV-A spectral ranges for the solar cycle 24 maximum (2012/2013) in W m^{-2}.

Wavelength	Ls 90	Ls 180	Ls 270	Ls 360
UV-C (200–280 nm)	2.0284	2.9864	3.1008	2.6390
UV-B (280–315 nm)	6.2971	9.2463	9.6242	8.1594
UV-A (315–400 nm)	25.8183	37.9033	39.567	33.6188

Table 2
Total daily irradiances in the UV-C, UV-B and UV-A spectral ranges for the solar cycle 24 minimum (2008/2009) in W m^{-2}.

Wavelength	Ls 90	Ls 180	Ls 270	Ls 360
UV-C (200–280 nm)	2.0100	2.9573	3.0789	2.6178
UV-B (280–315 nm)	6.2911	9.2736	9.6488	8.1984
UV-A (315–400 nm)	25.715	37.7878	39.4229	33.4826

Table 3
Spectral irradiance daily differences between maximum and minimum for Solar Cycle 24, calculated as $\frac{max-min}{max}\cdot 100$.

Wavelength	Ls 90	Ls 180	Ls 270	Ls 360
UV-C (200–280 nm)	0.9080%	0.9761 %	0.7042%	0.8036%
UV-B (280–315 nm)	0.0956%	−0.2958 %	−0.2555%	−0.4773 %
UV-A (315–400 nm)	0.3973%	0.3048 %	0.3652%	0.4052%

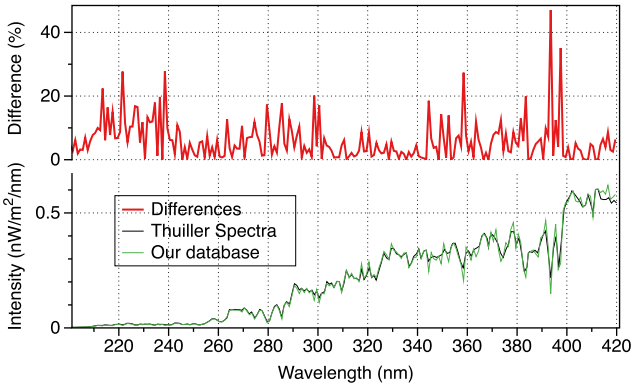

Fig. 3. Bottom: Comparison between Thuiller's generic spectra geometrically scaled to Mars position (black) and the spectra from our model (green) for Ls = 0° (2012/03/29). Top: Relative differences in % between our model and Thuiller Spectra calculated as $(\frac{Our\ model-Thuiller}{Our\ model}\cdot 100)$. Note the intensity differences at wavelengths 393 nm and 397 nm due to the Ca II K lines. (For interpretation of the references to color in this figure legend, the reader is referred to the web version of this article.)

Table 4
TOA irradiance with REMS UV-ABC (220–380 nm) surface measurements: Mars UV atmospheric absorption in the ABC band integrated range of 220–380 nm on Ls = 180 (sol 55 of MSL operation on Mars). The values correspond to Gale Crater on Mars, the Curiosity rover landing site.

TOA (220–380 nm) [W/m^2]	40.78
Global UV-ABC$_{max}$ (220–380 nm) at Gale [W/m^2]	19.45
Diffuse UV-ABC$_{max}$ (220–380 nm) at Gale [W/m^2]	3.28
SZA at maximum global irradiance	13
Estimated UV opacity	0.86

surface, after interacting with the atmospheric constituents, have been either scattered away from the direct path (and thus form part of the diffuse irradiance) or have been absorbed.

Table 4 shows an example of the UV radiative transfer properties of the atmosphere on Mars at the beginning local Spring (Ls 180) where the TOA UV-ABC (220–380 nm) irradiance is compared with the surface measured value global (i.e. direct plus diffuse) and diffuse UV irradiance.

With the knowledge of the radiation reaching the Top of the Atmosphere, it is possible to calculate the opacity of the atmosphere of Mars with an excellent precision. The estimated UV opacity for this sol is consistent with the reported visible opacity provided by the Mastcam solar observation of the Curiosity rover for this Ls, tau = 0.79–0.69, as well as the observed by the Opportunity rover (Lemmon, 2014).

3.2. Application to current and future surface missions to Mars

Here we present values for locations of special interest for present or future space exploration landing sites, including a prediction up to 2019, but values for other latitudes are located at https://atmospheres.research.ltu.se/ in the resources section. We have computed radiation values at the surface assuming an exponential attenuation with index $\tau = 0.3$, which is consistent with the minimum diode opacity (660-nm) measured by Viking missions in a clear scenario (this gives a value of the upper bound dose reaching the surface) (http://atmos.pds.nasa.gov).

3.2.1. Gale Crater (Curiosity landing site)

Tables 5 and 6 show the daily spectral irradiance average every 10 nm during the maximum (2012–2013) and the minimum (2008–2009) of the present solar cycle. The results in Tables 5 and 6 were calculated for the Gale Crater location (4.49°S, 137.42°E), the Curiosity rover landing site. Although the differences between the integrated spectral irradiance during the maximum and the minimum are of the order of 1%, those small variations could be very important in planetary sciences

Table 5
Daily irradiances in W m^{-2} nm^{-1} for solar cycle 24 maximum (2012/2013) at Gale.

Wavelength (nm)	Ls 90	Ls 180	Ls 270	Ls 360
1–10	1.1957×10^{-5}	2.3491×10^{-5}	1.2937×10^{-6}	1.6628×10^{-6}
10–20	2.1831×10^{-5}	3.6505×10^{-5}	5.4338×10^{-7}	1.1432×10^{-6}
20–30	2.2751×10^{-5}	4.0115×10^{-5}	4.7430×10^{-7}	8.2409×10^{-7}
30–40	2.4781×10^{-5}	4.0966×10^{-5}	7.0083×10^{-7}	1.1541×10^{-6}
40–50	5.1947×10^{-6}	8.3710×10^{-6}	4.0434×10^{-6}	3.6640×10^{-6}
50–60	4.1800×10^{-6}	6.5532×10^{-6}	5.7888×10^{-6}	5.1476×10^{-6}
60–70	3.7637×10^{-6}	5.9337×10^{-6}	5.4652×10^{-6}	4.8875×10^{-6}
70–80	4.0540×10^{-6}	6.3690×10^{-6}	5.9352×10^{-6}	5.2944×10^{-6}
80–90	9.5321×10^{-6}	1.4914×10^{-5}	1.4001×10^{-5}	1.2451×10^{-5}
90–100	1.1422×10^{-5}	1.7814×10^{-5}	1.6817×10^{-5}	1.4919×10^{-5}
100–110	1.0314×10^{-5}	1.6081×10^{-5}	1.5188×10^{-5}	1.3471×10^{-5}
110–120	8.0661×10^{-6}	1.2741×10^{-5}	1.1827×10^{-5}	1.0662×10^{-5}
120–130	2.4648×10^{-4}	3.8861×10^{-4}	3.5153×10^{-4}	3.2427×10^{-4}
130–140	4.2134×10^{-5}	6.6236×10^{-5}	6.0618×10^{-5}	5.5612×10^{-5}
140–150	2.0618×10^{-5}	3.1626×10^{-5}	3.0258×10^{-5}	2.6930×10^{-5}
150–160	4.4041×10^{-5}	6.7145×10^{-5}	6.4838×10^{-5}	5.7736×10^{-5}
160–170	9.5672×10^{-5}	1.4364×10^{-4}	1.4194×10^{-4}	1.2479×10^{-4}
170–180	2.8915×10^{-4}	4.3112×10^{-4}	4.3443×10^{-4}	3.7424×10^{-4}
180–190	7.9319×10^{-4}	1.1849×10^{-3}	1.1953×10^{-3}	1.0311×10^{-3}
190–200	1.5640×10^{-3}	2.3306×10^{-3}	2.3754×10^{-3}	2.0332×10^{-3}
200–210	3.1216×10^{-3}	4.6459×10^{-3}	4.7525×10^{-3}	4.0598×10^{-3}
210–220	9.8404×10^{-3}	1.4515×10^{-2}	1.5002×10^{-2}	1.2805×10^{-2}
220–230	1.4102×10^{-2}	2.0818×10^{-2}	2.1533×10^{-2}	1.8360×10^{-2}
230–240	1.3892×10^{-2}	2.0478×10^{-2}	2.1191×10^{-2}	1.8055×10^{-2}
240–250	1.5746×10^{-2}	2.3191×10^{-2}	2.4015×10^{-2}	2.0439×10^{-2}
250–260	2.2838×10^{-2}	3.3646×10^{-2}	3.4943×10^{-2}	2.9765×10^{-2}
260–270	5.4632×10^{-2}	8.0357×10^{-2}	8.3612×10^{-2}	7.1145×10^{-2}
270–280	6.3161×10^{-2}	9.2841×10^{-2}	9.6634×10^{-2}	8.2097×10^{-2}
280–290	7.6375×10^{-2}	0.1122	0.1166	9.9025×10^{-2}
290–300	0.1515	0.2224	0.2313	0.1959
300–310	0.1710	0.2512	0.2609	0.2208
310–320	0.2073	0.3044	0.3176	0.2698
320–330	0.2551	0.3744	0.3910	0.3321
330–340	0.2878	0.4225	0.4412	0.3748
340–350	0.2963	0.4349	0.4541	0.3858
350–360	0.3094	0.4543	0.4742	0.4029
360–370	0.3488	0.5119	0.5346	0.4542
370–380	0.3575	0.5248	0.5479	0.4655
380–390	0.3175	0.4664	0.4865	0.4135
390–400	0.3537	0.5196	0.5420	0.4606
400–410	0.5243	0.7694	0.8037	0.6827
410–420	0.5601	0.8220	0.8586	0.7293

Table 6
Daily irradiances in W m^{-2} nm^{-1} for solar cycle 24 minimum (2008/2009) at Gale.

Wavelength (nm)	Ls 90	Ls 180	Ls 270	Ls 360
1–10	4.0728×10^{-6}	6.2646×10^{-6}	6.9435×10^{-6}	6.0578×10^{-6}
10–20	1.5558×10^{-5}	2.3035×10^{-5}	2.4378×10^{-5}	2.0794×10^{-5}
20–30	1.3195×10^{-5}	1.9675×10^{-5}	2.1043×10^{-5}	1.8021×10^{-5}
30–40	1.8349×10^{-5}	2.7143×10^{-5}	2.8676×10^{-5}	2.4452×10^{-5}
40–50	3.8860×10^{-6}	5.7577×10^{-6}	6.0942×10^{-6}	5.2234×10^{-6}
50–60	3.3885×10^{-6}	5.0180×10^{-6}	5.3005×10^{-6}	4.5510×10^{-6}
60–70	3.0317×10^{-6}	4.4965×10^{-6}	4.7554×10^{-6}	4.0921×10^{-6}
70–80	3.3289×10^{-6}	4.9339×10^{-6}	5.2127×10^{-6}	4.4819×10^{-6}
80–90	7.7400×10^{-6}	1.1465×10^{-5}	1.2114×10^{-5}	1.0409×10^{-5}
90–100	9.4749×10^{-6}	1.4026×10^{-5}	1.4803×10^{-5}	1.2708×10^{-5}
100–110	8.5557×10^{-6}	1.2664×10^{-5}	1.3366×10^{-5}	1.1474×10^{-5}
110–120	7.2429×10^{-6}	1.0868×10^{-5}	1.1211×10^{-5}	9.6939×10^{-6}
120–130	1.9776×10^{-4}	2.9122×10^{-4}	3.1113×10^{-4}	2.6709×10^{-4}
130–140	3.5155×10^{-5}	5.1873×10^{-5}	5.4895×10^{-5}	4.7264×10^{-5}
140–150	1.8758×10^{-5}	2.7998×10^{-5}	2.9094×10^{-5}	2.4881×10^{-5}
150–160	4.0296×10^{-5}	5.9741×10^{-5}	6.2091×10^{-5}	5.3475×10^{-5}
160–170	8.9947×10^{-5}	1.3292×10^{-4}	1.3851×10^{-4}	1.1870×10^{-4}
170–180	2.8147×10^{-4}	4.1383×10^{-4}	4.3165×10^{-4}	3.6680×10^{-4}
180–190	7.6224×10^{-4}	1.1172×10^{-3}	1.1730×10^{-3}	1.0000×10^{-3}
190–200	1.5131×10^{-3}	2.2226×10^{-3}	2.3213×10^{-3}	1.9752×10^{-3}
200–210	3.0230×10^{-3}	4.4491×10^{-3}	4.6440×10^{-3}	3.9500×10^{-3}
210–220	9.6697×10^{-3}	1.4219×10^{-2}	1.4824×10^{-2}	1.2604×10^{-2}
220–230	1.3886×10^{-2}	2.0440×10^{-2}	2.1299×10^{-2}	1.8117×10^{-2}
230–240	1.3722×10^{-2}	2.0189×10^{-2}	2.1019×10^{-2}	1.7871×10^{-2}
240–250	1.5635×10^{-2}	2.2984×10^{-2}	2.3920×10^{-2}	2.0323×10^{-2}
250–260	2.2480×10^{-2}	3.3100×10^{-2}	3.4487×10^{-2}	2.9354×10^{-2}
260–270	5.4213×10^{-2}	7.9758×10^{-2}	8.3016×10^{-2}	7.0605×10^{-2}
270–280	6.2931×10^{-2}	9.2586×10^{-2}	9.6358×10^{-2}	8.1864×10^{-2}
280–290	7.6470×10^{-2}	0.1125	0.1170	9.9431×10^{-2}
290–300	0.1522	0.2242	0.2331	0.1979
300–310	0.1711	0.2531	0.2627	0.2232
310–320	0.2060	0.3032	0.3162	0.2688
320–330	0.2535	0.3731	0.3890	0.3305
330–340	0.2863	0.4211	0.4388	0.3730
340–350	0.2946	0.4333	0.4520	0.3839
350–360	0.3076	0.4523	0.4719	0.4010
360–370	0.3474	0.5105	0.5327	0.4523
370–380	0.3560	0.5229	0.5458	0.4635
380–390	0.3167	0.4650	0.4855	0.4121
390–400	0.3535	0.5188	0.5414	0.4595
400–410	0.5234	0.7681	0.8016	0.6807
410–420	0.5590	0.8204	0.8561	0.7270

(McKenzie et al., 2003). These differences should be larger under high solar activity conditions. During a solar cycle, the total solar spectral irradiance variation is about 0.1%, but individual wavelengths could change their irradiance up to 60% (Krivova et al., 2006), as can be seen in Fig. 3 as a consequence for example of the Ca II K lines explained before.

3.2.2. Elysium Planitia (Insight landing site)

Table 7 shows the averaged spectral irradiance for the Martian year 34 (2017/2018) in the Elysium Planitia area every 10 nm (from 2.5°S to 4°N). This is the selected landing site for NASA's Insight mission in 2016. Table 7 represents a useful tool to predict the spectral irradiance on the area, important for scientific and engineering studies. More information about the landing site could be found in Golombek et al. (2013).

Fig. 4 shows the UV radiation on Mars TOA in the 200–400 nm spectral region for a complete orbit at the Martian year 31 (2011/2013). The maximum value of the integrated radiation in the 200–400 nm interval on Mars is about 50 W/m^2, and is located in the zone near −23° as a consequence of the eccentricity of the planet. This radiation map of Mars TOA is correlated with the radiation reaching the surface. The knowledge of the UV radiation at TOA along with the absorbers in the atmosphere allows the study of the radiation field at surface.

4. Conclusions

UV radiation reaching Mars TOA has been computed for solar cycle 24 (2008–2019), based on real data provided by the SORCE mission and predicted values of solar radio flux F10.7 in a modified version of the Woods–Rottman model. We present a database divided in two sections: with real data extrapolated to Mars (2008–2013) and predicted values based on the F10.7 index (2014–2019).

This database allows to take into account the effects of the solar cycle in the UV radiation. The changes at particular wavelengths could be up to 50%, and variations are usually between 5% and 20%.

Using the computed TOA values and the UV radiation measured by the REMS instrument on the Curiosity rover we have computed, as an academic example, the UV opacity for a particular day of REMS measurements. We obtain a value of the UV opacity (0.89) consistent with other measurements on Mars.

The Solar radiation is not completely isotropic. In order to eliminate the perturbations derived from a particular location, we present averaged values of 3, 7 and 15 days, which provides a much better representation to the current stage in the solar cycle than generic spectra used nowadays.

The knowledge of UV radiation on Mars TOA allows the study of surface and atmospheric events on Mars. This database provides a tool for scientific and engineering investigations on Mars based on

Table 7
Daily irradiances in W m^{-2} nm^{-1} for Mars for Martian year 34 (2017/2018) in Elysium Planitia.

Wavelength (nm)	Ls 90	Ls 180	Ls 270	Ls 360
1–10	6.5763×10^{-6}	4.9452×10^{-6}	5.9300×10^{-6}	5.7179×10^{-6}
10–20	2.3931×10^{-5}	1.8530×10^{-5}	2.4881×10^{-5}	2.4537×10^{-5}
20–30	1.9097×10^{-5}	1.4675×10^{-5}	1.8375×10^{-5}	1.8007×10^{-5}
30–40	3.3905×10^{-5}	2.6371×10^{-5}	3.4462×10^{-5}	3.4061×10^{-5}
40–50	6.3460×10^{-6}	4.9513×10^{-6}	6.5544×10^{-6}	6.4917×10^{-6}
50–60	4.8357×10^{-6}	3.7965×10^{-6}	5.1708×10^{-6}	5.1421×10^{-6}
60–70	4.2881×10^{-6}	3.3589×10^{-6}	4.5843×10^{-6}	4.5529×10^{-6}
70–80	4.6684×10^{-6}	3.6618×10^{-6}	5.0176×10^{-6}	4.9873×10^{-6}
80–90	1.0877×10^{-5}	8.5413×10^{-6}	1.1661×10^{-5}	1.1598×10^{-5}
90–100	1.3214×10^{-5}	1.0390×10^{-5}	1.4247×10^{-5}	1.4181×10^{-5}
100–110	1.1931×10^{-5}	9.3822×10^{-6}	1.2864×10^{-5}	1.2805×10^{-5}
110–120	7.2786×10^{-6}	5.7508×10^{-6}	7.9908×10^{-6}	7.9765×10^{-6}
120–130	2.7770×10^{-4}	2.1865×10^{-4}	2.9939×10^{-4}	2.9823×10^{-4}
130–140	4.8790×10^{-5}	3.8475×10^{-5}	5.3017×10^{-5}	5.2862×10^{-5}
140–150	2.5287×10^{-5}	2.0050×10^{-5}	2.7994×10^{-5}	2.8000×10^{-5}
150–160	5.4408×10^{-5}	4.3215×10^{-5}	6.0614×10^{-5}	6.0687×10^{-5}
160–170	1.2009×10^{-4}	9.5646×10^{-5}	1.3460×10^{-4}	1.3496×10^{-4}
170–180	3.6978×10^{-4}	2.9500×10^{-4}	4.1593×10^{-4}	4.1744×10^{-4}
180–190	1.0066×10^{-3}	8.0310×10^{-4}	1.1313×10^{-3}	1.1354×10^{-3}
190–200	1.9931×10^{-3}	1.5913×10^{-3}	2.2430×10^{-3}	2.2521×10^{-3}
200–210	3.9843×10^{-3}	3.1817×10^{-3}	4.4871×10^{-3}	4.5057×10^{-3}
210–220	1.2652×10^{-2}	1.0119×10^{-2}	1.4274×10^{-2}	1.4345×10^{-2}
220–230	1.8178×10^{-2}	1.4541×10^{-2}	2.0524×10^{-2}	2.0628×10^{-2}
230–240	1.7922×10^{-2}	1.4334×10^{-2}	2.0234×10^{-2}	2.0335×10^{-2}
240–250	2.0364×10^{-2}	1.6290×10^{-2}	2.2998×10^{-2}	2.3115×10^{-2}
250–260	2.9474×10^{-2}	2.3588×10^{-2}	3.3320×10^{-2}	3.3498×10^{-2}
260–270	7.0789×10^{-2}	5.6673×10^{-2}	8.0085×10^{-2}	8.0528×10^{-2}
270–280	8.1965×10^{-2}	6.5621×10^{-2}	9.2731×10^{-2}	9.3245×10^{-2}
280–290	9.9320×10^{-2}	7.9516×10^{-2}	0.1123	0.1129
290–300	0.1973	0.1580	0.2233	0.2246
300–310	0.2224	0.1781	0.2517	0.2532
310–320	0.2728	0.2185	0.3088	0.3105
320–330	0.3347	0.2680	0.3788	0.3810
330–340	0.3762	0.3013	0.4258	0.4283
340–350	0.3787	0.3033	0.4287	0.4311
350–360	0.3872	0.3101	0.4383	0.4408
360–370	0.4517	0.3617	0.5112	0.5142
370–380	0.4685	0.3752	0.5302	0.5333
380–390	0.3993	0.3197	0.4519	0.4545
390–400	0.4164	0.3335	0.4713	0.4740
400–410	0.6771	0.5423	0.7664	0.7708
410–420	0.7105	0.5691	0.8042	0.8088

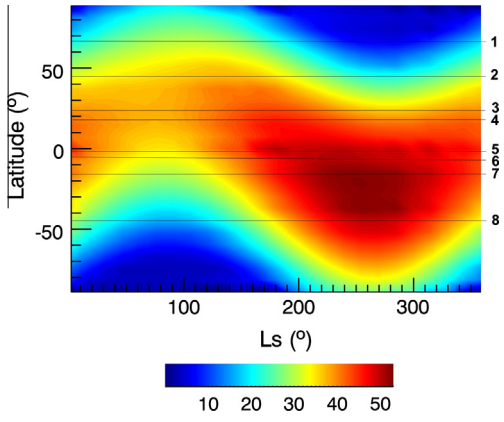

Fig. 4. Integrated UV radiation between 200 and 400 nm (W/m^2) map on Mars TOA for the 2011/2013 complete orbit based on SORCE data geometrically scaled to Mars position. Marked in the figure are Mars mission landing latitudes 1: Phoenix (68 N), 2: Viking 2 (48 N), 3: Viking 1 (23 N), 4: Pathfinder (19.30 N), 5: Opportunity (−1.9S), 6: Curiosity (−4.5S), 7: Spirit (−14.5) and 8: Mars 3 (45S).

real data instead of temporally static tabulated spectra. The full daily database between 10 and 420 nm every 1 nm at different latitudes is freely available at https://atmospheres.research.ltu.se/ in the resources section, as well as the averaged 3, 7, and 15 days databases, and will be periodically updated with the newest datasets.

Acknowledgements

The first author wants to acknowledge the Luleå University of Technology in Kiruna, Sweden, for the scholarship award that partially funded this investigation. We also thanks to Tom Woods for providing the W–R model and to him and Jeffrey Harder for their comments about the gaps and status of the SORCE data.

References

Ball, W.T., Unruh, Y.C., Krivova, N.A., Solanki, S., Harder, J.W., 2011. Solar irradiance variability: a six-year comparison between SORCE observations and the SATIRE model. Astron. Astrophys. 530, A71.

Boucher, N., Prezelin, B.B., Evens, T., Jovine, R., Kroon, B., Moline, M.A., Schofield, O., 1994. Icecolors '93: biological weighting function for the ultraviolet inhibition of carbon fixation in a natural antarctic phytoplankton community. Antarct. J. Rev. 1994, 272–275.

Ermolli, I., Matthes, K., Dudok de Wit, T., Krivova, N.A., Tourpali, K., Weber, M., Unruh, Y.C., Gray, L., Langematz, U., Pilewskie, P., Rozanov, E., Schmutz, W., Shapiro, A., Solanki, S.K., Thuillier, G., Woods, T.N., 2012. Recent variability of the solar spectral irradiance and its impact on climate modelling. Atmos. Chem. Phys. Discuss. 12, 24557–24642.

ftp://ftp.swpc.noaa.gov/pub/weekly/Predict.txt.

Ghetti, F., Checcucci, G., Bornman, J.F., 2006. Environmental UV radiation: impact on ecosystems and human health and predictive models. Nato Sci. Ser. 57, 288.

Golombek, M., Redmond, L., Gengl, H., Schwartz, C., Warner, N., Banerdt, B., Smrekar, S., 2013. Selection of the Insight landing site: constrains, plans, and progress. In: 44th Lunar and Planetary Science Conference. 1691 (abstract).

Gómez-Elvira, J., Armiens, C., Castaner, L., Domínguez, M., Genzer, M., Gómez, F., Haberle, R., Harri, A.-M., Jimenez, V., Kahanpää, H., Kowalski, L., Lepinette, A., Martínez-Frías, J., Martín, J., McEwan, I., Mora, L., Moreno, J., Navarro, S., de Pablo, M.A., Peinado, V., Pena, A., Polkko, J., Ramos, M., Renno, N.O., Ricart, J., Richardson, M., Rodríguez-Manfredi, J., Romeral, J., Sebastián, E., Serrano, J., de la Torre Juárez, M., Torres, J., Torrero, F., Urqui, R., Velasco, T., Verdasca, J., Zorzano, M.-P., Martín-Torres, F.J., 2012. REMS: an environmental sensor suite for the mars science laboratory. Space Sci. Rev. 170, 556.

Gómez-Elvira, J., Armiens, C., Carrasco, I., Genzer, M., Gómez, F., Haberle, R., Hamilton, V.E., Harri, A-M., Kahanpää, H., Kemppinen, O., Lepinette, A., Martín-Soler, J., Martń-Torres, J., Martínez-Frías, J., Mischna, M., Mora, L., Navarro, S., Newman, C., de Pablo, M.A., Peinado, V., Polkko, J., Rafkin, S.C.R., Ramos, M., Rennó, N.O., Richardson, M., Rodríguez-Manfredi, J.A., Romeral Planelló, J.J., Sebastián, E., de la Torre Juárez, M., Torres, J., Urquí, R., Vasavada, A.R., Verdasca, J., Zorzano, M.-P., 2014. Curiosity's rover environmental monitoring station: overview of the first 100 sols. J. Geophys. Res.: Planets. http://dx.doi.org/10.1002/2013JE004576 (in press).

Häder, D.P., Kumar, H.D., Smithc, R.C., Worrestd, R.C., 2007. Effects of solar UV radiation on aquatic ecosystems and interactions with climate change. Photochem. Photobiol. Sci. 6, 267–285.

Häder, D.P., Helbling, E.W., Williamson, C.E., Worrest, R.C., 2011. Effects of UV radiation on aquatic ecosystems and interactions with climate change. Photochem. Photobiol. Sci. 10, 242–260.

http://atmos.pds.nasa.gov.

Keppler, F., Vigano, I., McLeod, A., Ott, U., Frchtl, M., Rckmann, T., 2012. Ultraviolet-radiation-induced methane emissions from meteorites and the Martian atmosphere. Nature 486, 93–96.

Krivova, N.A., Solanki, S.K., Floyd, L., 2006. Reconstruction of solar UV irradiance in cycle 23. Astron. Astrophys. 452, 631–639.

Lemmon, M.T., 2014. The Mars Science Laboratory optical depth record. In: Eighth International Conference on Mars. 1338 (abstract).

Levine, J.S., Kraemer, D.R., Kuhn, W.R., 1977. Solar radiation incident on Mars and the outer planets: latitudinal, seasonal, and atmospheric effects. Icarus 31, 136–145.

Lindberg, C., Horneck, G., 1991. Action spectra for survival and spore photoproduct formation of Bacillus subtilis irradiated with short-wavelength (200–300 nm) UV at atmospheric pressure and in vacuo. J. Photochem. Photobiol. B: Biol. 11, 69–80.

McKenzie, R.L., Bjorn, L.O., Bais, A., Ilyasd, M., 2003. Changes in biologically active ultraviolet radiation reaching the Earth's surface. Photochem. Photobiol. Sci. 2, 5–15.

Merkel, A.W., Harder, J.W., Marsh, D.R., Smith, A.K., Fontenla, J.M., Woods, T.N., 2011. The impact of solar spectral irradiance variability on middle atmospheric ozone. Geophys. Res. Lett. 38, L13802. http://dx.doi.org/10.1029/2011GL047561.

Pankratz, C.K., Knapp, B.G., Fontenla, J.M., Rottman, G.J., Woods, T.N., Harder, J.W., Kopp, G., McClintock, W.E., Snow, M., 2005. SORCE solar irradiance data products. In: AGU Spring Meeting Abstracts, p. B3.

Rottman, G., 2005. The SORCE mission. In: Rottman, G., Woods, T., George, V. (Eds.), The Solar Radiation and Climate Experiment (SORCE). Springer, New York, pp. 7–25.

Rottman, G.J., Woods, T.N., McClintock, W., 2006. SORCE solar UV irradiance results. Adv. Space Res. 37, 201–208.

Thuillier, G., Hersé, M., Labs, D., Foujols, T., Peetermans, W., Gillotay, D., Simon, P.C., Mandel, H., 2003. The solar spectral irradiance from 200 to 2400 nm as measured by the SOLSPEC spectrometer from the ATLAS and EURECA missions. Sol. Phys. 214, 1–22.

Woods, T.N., Rottman, G.J., 2002. Solar ultraviolet variability over time periods of aeronomic interest. In: Mendillo, M., Nagy, A., Hunter Waite, J., Jr. (Eds.), Atmospheres in the Solar System: Comparative Aeronomy, Geophys. Monogr. Ser., vol. 130. AGU, Washington, D.C., pp. 221–234.